Optical and photoluminescent properties of nanostructured hybrid films based on functional fullerenes and metal nanoparticles

N. Dmitruk[1], O. Borkovskaya[1], D. Naumenko[1], N. Berezovska[2], I. Dmitruk[2], V. Meza-Laguna[3], E. Alvarez-Zauco[3], E. Basiuk[3,4]
[1]*Institute of Semiconductor Physics, NAS of Ukraine, 45, prospect Nauky, 03028 Kyiv, Ukraine*
[2]*Taras Shevchenko Kyiv National University, Experimental Physics Department,*
64, Volodymyrs'ka str., 01601 Kyiv, Ukraine
[3]*Centro de Ciencias Aplicadas y Desarrollo Tecnológico, Universidad Nacional Autónoma de México, Circuito Exterior C.U., 04510 México, D.F., Mexico*
[4]*School of Materials Science and Engineering, University of New South Wales, Sydney 2052, Australia*

Abstract. The chemically cross-linked C_{60} thin films, capable of binding Ag or Au nanoparticles, were prepared by the gas-phase treatment with diamine for one set of samples and dithiol for another one and decoration with Ag or Au nanoparticles, respectively. The optical and photoluminescent properties of the obtained nanostructured hybrid films in comparison with the undecorated films were studied. The low temperature photoluminescence (PL) spectra demonstrate significant changes of the band intensity and appearance of fine structure for bands connected with radiative transitions of self-trapped and localized excitons. The decoration of pristine and treated C_{60} films with Ag nanoparticles leads to a decrease of PL intensity and to slight bandgap reduction. These phenomena can be explained by the increase of the surface recombination velocity at the fullerene-nanoparticle interface. At the same time, the nanoparticles insignificantly decrease the transmittance of light into the fullerene and Si layers, and have almost no influence on photoelectric properties of metal/fullerene/Si barrier structures.

Keywords: fullerene C_{60}, thin film, functionalization, octane-1,8-diamine, octane-1,8-dithiol, silver nanoparticles, gold nanoparticles, optical, photoelectric.

1. Introduction

The development of different fullerene-based materials is stimulated by considerable potential for application in nanoelectronic devices. In particular, due to the special structural and chemical characteristics, C_{60} molecules in combination with metals are promising for creation of novel nanohybrid materials with unique catalytic, optical and photoelectric properties [1-3]. Thus, fullerene films provide a wide range of bonding sites which could be exploited as molecular templates. Different organic cross-linkers resulted to be very attractive to assemble nanoparticles in the formation of covalently linked superstructures. The cross-linking molecules with spacers of various lengths allows to control, to some extent, over interparticle spacing, and in its turn, the interparticle spacing influences the material properties such as conductivity. We applied the direct solvent-free functionalization of C_{60} films with aliphatic bifunctional amines and thiols, such as octane-1,8-diamine and octane-1,8-dithiol, to prepare covalently functionalized, cross-linked fullerene supports capable of strong binding and immobilization of noble metal (e.g., silver and gold) nanoparticles [4, 5]. However, the properties of fullerene thin films depend considerably on the interface configuration, and the study of the absorption and luminescence behavior, charge transfer interactions of fullerene with the metal surface is of crucial importance.

In the present work, we report on a detailed study of optical and photoelectric properties of two series of pristine and chemically functionalized fullerene specimens based on the C_{60} films deposited on *n*-silicon substrates. This set of experimental methods allows to study both radiative and non-radiative recombination influences on photoresponse of fullerite films. The first series of samples consists of (i) pristine fullerene films (C_{60}/Si), (ii) 1,8-diaminooctane-crosslinked C_{60} films (C_{60}-DA/Si), (iii) pristine films decorated with Ag

nanoparticles (C_{60}-Ag/Si), and (iv) cross-linked films decorated with Ag nanoparticles (C_{60}-DA-Ag/Si), and second series includes (i) pristine fullerene films (C_{60}/Si), (ii) octane-1,8-dithiol-crosslinked C_{60} films (C_{60}-DT/Si), (iii) pristine films decorated with Au nanoparticles (C_{60}-Au/Si), and (iv) cross-linked films decorated with Au nanoparticles (C_{60}-DT-Au/Si).

2. Experimental details

C_{60} films were deposited on silicon Si (100) wafers by sublimation method. The deposition was performed in a vacuum chamber at the pressure of 6.2×10^{-6} Torr, without heating the substrates. The average thickness of obtained film was about 100 nm.

The gas-phase solvent-free procedure has been employed for functionalization of deposited fullerene films with aliphatic bifunctional amines and thiols, such as octane-1,8-diamine and octane-1,8-dithiol. The Ag and Au nanoparticle deposition is based on the reduction of $AgNO_3$ or $HAuCl_4$ with citric acid, respectively. The

details concerning the samples preparation and analysis of their structure were reported formerly [4-6].

To characterize photoelectric properties of obtained fullerene/Si heterostructures, photodiodes were fabricated by evaporation of a semitransparent gold electrode layer (thickness of 22.7 nm) through an opaque mask (opening diameter of 1.3 mm) onto pristine and functionalized C_{60} films, and by making an ohmic contact to the rear side of Si substrate. These samples are referred to as metal(Au)/C_{60}/Si, metal(Au)/C_{60}-DA/Si, metal(Au)/C_{60}-Ag/Si, and metal(Au)/C_{60}-DA-Ag/Si.

3. Results and discussion

The investigation of structure and morphology of fullerene films before and after deposition of Ag nanoparticles was carried out by means of high-resolution transmission electron microscopy (HRTEM). As it is shown in Fig. 1a, pristine C_{60} film deposited onto a TEM grid exhibits mainly an amorphous structure, with the presence of dispersed crystalline regions. The morphology
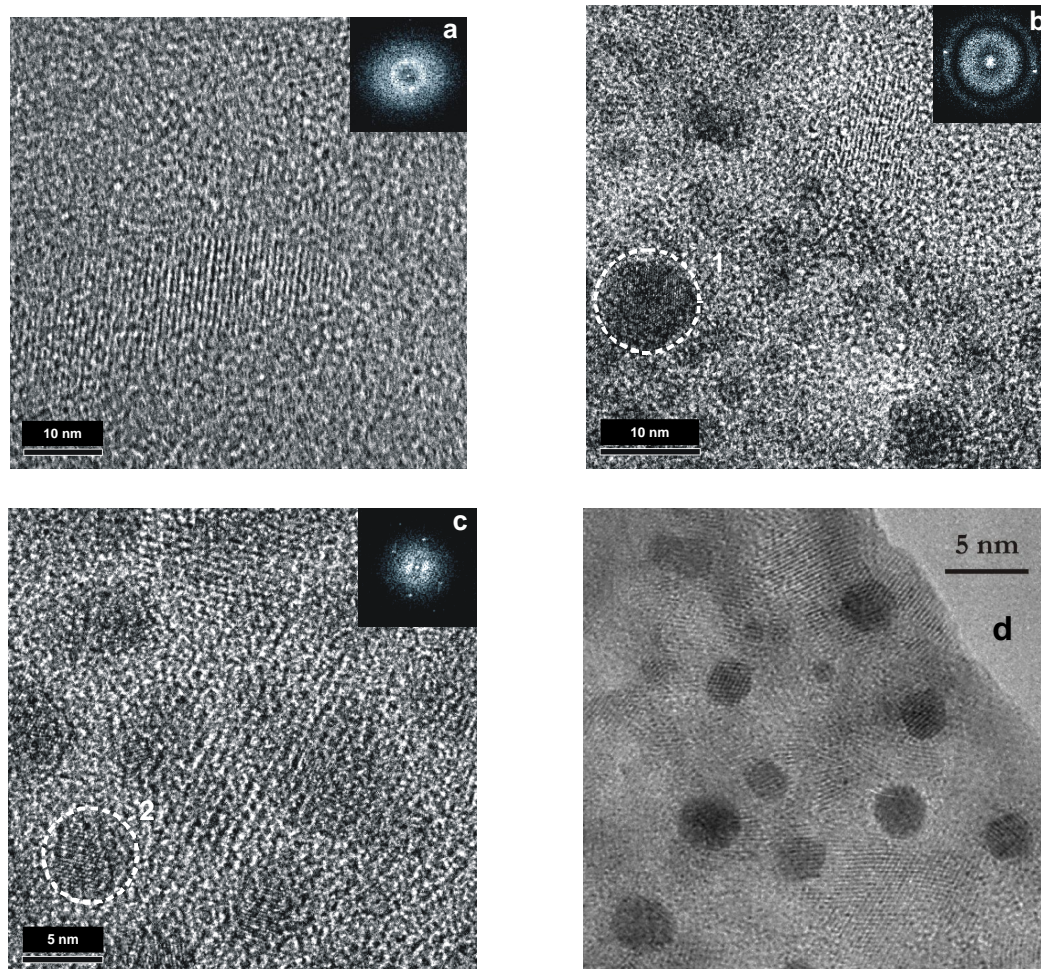
Fig. 1. HRTEM images of (a) pristine C_{60} before the deposition of silver nanoparticles, Ag nanoparticles deposited onto (b) pristine and (c) 1,8-diaminooctane-functionalized C_{60}. Insets show selected area electron diffraction patterns for (a) pristine C_{60} and (b, c) Ag nanoparticles marked with numbered white circles; (d) HRTEM images of 1,8-dithiloctane-functionalized C_{60} with Au nanoparticles.

of silver nanoparticles deposited onto the TEM grid-supported pristine and diamine-functionalized C_{60} films is exemplified in Fig. 1b, c, respectively, where the insets correspond to electron diffraction patterns of the particles marked with white circles. Four diffraction planes, namely (111), (200), (222), and (311), were identified in the case of Ag on pristine C_{60}, whereas only (111) and (222) planes were clearly observed for typical Ag nanoparticles on the diamine-functionalized C_{60}. The Ag particle size dispersion was narrower, as well as the coverage was more uniform, in the case of 1,8-diaminooctane-functionalized C_{60}, as compared to pristine fullerene. The particles of about 5 nm in diameter were typically observed on the functionalized C_{60}, whereas they had much more variable sizes when deposited onto pristine C_{60}. For octane-1,8-dithiol-functionalized films (Fig. 1d), the Au particle sizes exhibited a narrow dispersion. The particles of about 3 nm in diameter were commonly observed on the dithiol-functionalized C_{60} films.

For optical characterization of investigated structures, the reflectance spectra were measured in the energy range of $h\nu = 1.1$-3.1 eV at variable angles of incidence of *p*- and *s*-polarized light. The fullerene layer thickness value and its optical parameters (refractive index *n*, and extinction coefficient *k* at complex refractive index $\check{n} = n - ik$) were determined by fitting of experimental dependences with theoretical ones, calculated within the framework of a one-layer model for pristine or functionalized C_{60} films. To confirm these results, the ellipsometric measurements were performed using a Woollam M2000DI rotating compensator ellipsometer in the spectral range of 1.55-5 eV, at angles of incidence of 45°, 60°, 65°, and 75° for C_{60}-DT-Au/Si structure (Fig. 2). The obtained parameters allowed to calculate the spectral dependences of the absorption coefficient ($\alpha = 4\pi k/\lambda$) (Figs 3 and 4) and the spectra of light transmittance into Si substrate through Au, C_{60} and Au/C_{60} layers, which are used later for calculating the internal quantum efficiency spectra.
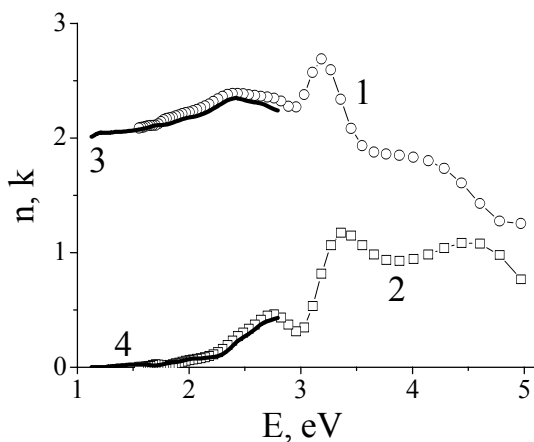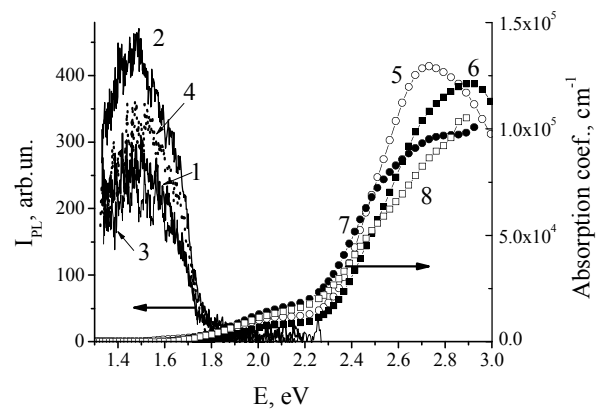
Photoluminescence (PL) spectra were studied with a grating monochromator MDR-3 at room and low (77 and 2 K) temperatures under Ar ion laser (488 nm) excitation.

At room temperature, for samples of series 1 we have observed the wide structureless asymmetric PL band with maximum in the vicinity of 1.5 eV (Fig. 3). The intensity of PL spectrum of diamine-functionalized film was higher than for pristine fullerene film. The intensity of PL spectra of pristine and cross-linked films decorated with Ag nanoparticles depends on the place of the excitation spot on the sample. As for series 2, the PL spectra demonstrated two strongly overlapped bands with pronounced maxima at 1.51 and 1.67 eV (according to the multi-peak analysis) (Fig. 4).

The PL spectra of samples of series 1 at 77 K are shown in Fig. 5. Experimental PL spectra have been approximated with a sum of Gaussian bands. Such fitting allows to determine the spectral position (x_i) of the bands more precisely (Table). The band positions are in agreement with the values reported for C_{60} solid films measured at 100 K [7] and 80 K [8]. A slight red shift of PL bands observed for C_{60}-DA/Si film relative to the pristine one is characteristic for photopolymerized C_{60} solid films [7, 8] and is consistent with our earlier results for photopolymerized and chemically cross-linked fullerenes [9]. Chemical cross-linking of C_{60} molecules removes the degeneracies of the electronic energy levels in the C_{60} monomers. The pristine fullerene films are typically composed of well-shaped C_{60} clusters of the approximately 50 nm average diameter. Their edges became notably diffuse after the modification with diamine [4]. These changes can be explained by the formation of covalent cross-links between neighboring fullerene molecules and clusters: since the diamine linkers are relatively big and cannot fit the spaces between C_{60} molecules, the latter had to reaccommodate, thus making the film less dense and ordered.

Fig. 2. The dispersion of refractive index *n* (*1, 3*) and extinction coefficient *k* (*2, 4*) for C_{60}-DT-Au film on Si substrate. The results obtained from the ellipsometric measurements (*1, 2*), and from reflectance measurements (*3, 4*).

Fig. 3. The photoluminescence (*1-4*) and absorption coefficient (*5-8*) spectra for structures of series 1: pristine C_{60} layer (*1, 5*), C_{60}-DA (*2, 6*), C_{60}-Ag (*3, 7*) and C_{60}-DA-Ag (*4, 8*). $\lambda_{excPL} =$ 488.0 nm, $T = 300$ K.
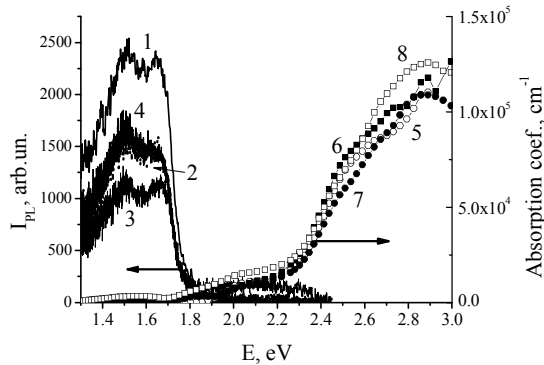
Fig. 4. The photoluminescence (*1-4*) and absorption coefficient (*5-8*) spectra for structures of series 2: pristine C_{60} layer (*1, 5*), C_{60}-DT (*2, 6*), C_{60}-Au (*3, 7*) and C_{60}-DT-Au (*4, 8*). $\lambda_{excPL} = 488.0$ nm, $T = 300$ K.

Table. The spectral positions (x_i) of Gaussian bands in PL spectra of pristine and functionalized fullerene films, with and without deposited metal nanoparticles.

Band	C_{60}/Si x_1, eV	C_{60}-DA/Si x_2, eV	C_{60}-Ag/Si x_3, eV	C_{60}-DA-Ag/Si x_4, eV
		Series 1, $T = 77$ K		
I	1.696	1.695	1.690	1.689
II	1.659	1.658	1.651	1.652
III	1.615	1.619	1.620	1.617
IV	1.570	1.574	1.584	1.579
V	1.517	1.517	1.531	1.523
VI	1.471	1.471	1.488	1.482
VII	1.418	1.418	1.436	1.431
VIII	1.358	1.360	1.379	1.374
		Series 1, $T = 2$ K		
I	1.695	1.704	1.704	1.699
II	1.658	1.685	1.679	1.658
III	1.621	1.617	1.609	1.603
IV	1.580	1.521	1.522	1.533
V	1.516	1.480	1.456	1.483
VI	1.454	1.440	1.402	1.430
VII	1.398	1.386	1.348	1.359
VIII	1.326	1.319	1.300	1.300

| Band	C_{60}/Si x_1, eV	C_{60}-DT/Si x_2, eV	C_{60}-Au/Si x_3, eV	C_{60}-DT-Au/Si x_4, eV
		Series 2, $T = 77$ K		
I	1.711	1.699	1.702	1.701
II	1.682	1.670	1.665	1.668
III	1.638	1.629	1.625	1.601
IV	1.591	1.585	1.585	1.539
V	1.529	1.523	1.532	1.501
VI	1.491	1.487	1.486	1.444
VII	1.429	1.436	1.432	1.372
VIII	1.331	1.331	1.330	1.300
		Series 2, $T = 2$ K		
I	1.708	1.705	1.705	1.702
II	1.678	1.675	1.667	1.669
III	1.631	1.625	1.623	1.610
IV	1.587	1.583	1.587	1.554
V	1.532	1.528	1.534	1.504
VI	1.482	1.487	1.487	1.442
VII	1.419	1.421	1.422	1.365
VIII	1.336	1.336	1.335	1.300
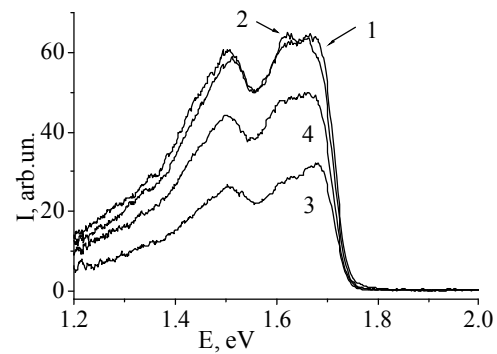
Fig. 5. Photoluminescence spectra of C_{60}/Si (*1*), C_{60}-DA/Si (*2*), C_{60}-Ag/Si (*3*) and C_{60}-DA-Ag/Si (*4*), $\lambda_{exc} = 488.0$ nm, $T = 77$ K.

The decoration of fullerene films with Ag nanoparticles results in an additional red shift of PL bands (see Table), which correlates with the decrease of the band gap values. Similar effect was also reported by other authors [10, 11]. Besides, the PL band intensities for the functionalized C_{60} samples are redistributed. The diamine treatment increases intensities of the bands below 1.689 eV, whereas the Ag decoration decreases them. It should be mentioned that the interaction of Ag core with pristine C_{60} molecules, which do not have nitrogen donor atoms capable of stable silver coordination, is weaker as compared to the diamine-functionalized fullerene. In the latter case, the newly formed Ag nanoparticles remain strongly coordination bound to the NH bridges (and to the existing unreacted NH_2 groups), which are separated by a considerable distance from each other, and thus immobilized. On the contrary, the silver core keeps their mobility on pristine C_{60}, and therefore can undergo gradual coalescence increasing their size and forming twins. The PL band at 1.689 eV (Fig. 5) can be attributed to the radiative recombination of self-trapped polaron excitons [12]. This exciton can be considered as a Frenkel exciton trapped by lattice deformation. Bands at lower energies are due to the emission from the so-called X traps [13], or defects presumably associated with the grain boundaries [8]. Likewise the case of photopolymerized C_{60} solid films [7, 8, 14], the observed changes of PL band position and intensity due to the 1,8-diaminooctane functionalization can be explained by a transformation of shallow traps into deeper traps caused by the perturbation of icosahedral shell symmetry of C_{60} molecules and activation of new vibrational and electronic states in the cross-linked films. The decrease of all PL bands intensities after the deposition of Ag nanoparticles can be explained by an increase of the non-radiative surface recombination velocity at the fullerene-Ag interface.

The main features of PL spectra of the samples of series 2 are similar to those in the spectra of series 1 (Fig. 6). However, the intensity of PL spectrum of dithiol-functionalized C_{60} film is considerably lower in comparison with the pristine C_{60} film spectrum. It is the
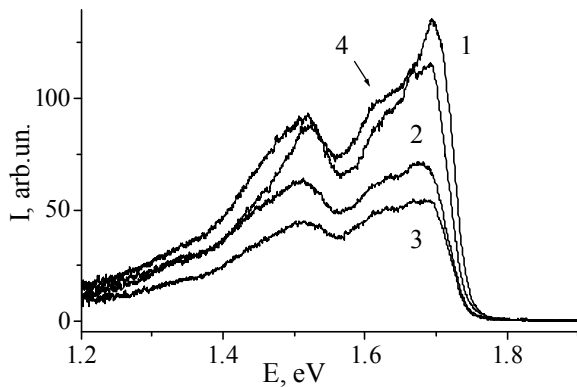
Fig. 6. Photoluminescence spectra of C_{60}/Si (*1*), C_{60}-DT/Si (*2*), C_{60}-Au/Si (*3*) and C_{60}-DT-Au/Si (*4*), λ_{exc} = 488.0 nm, T = 77 K.
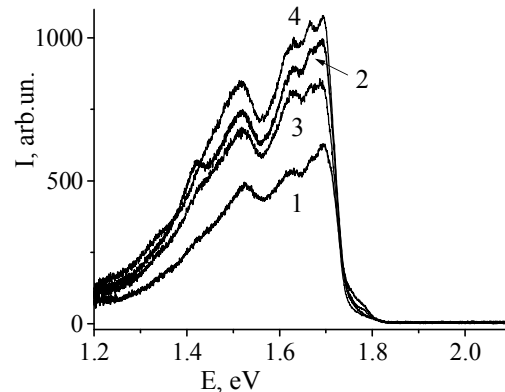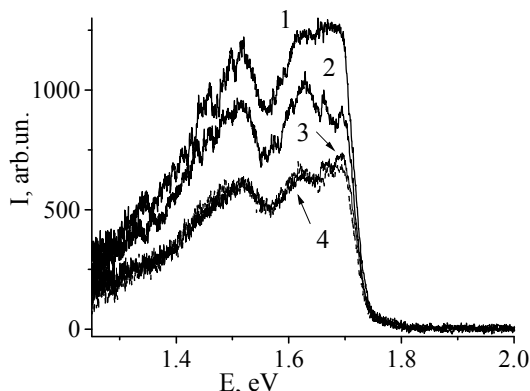

Fig. 8. Photoluminescence spectra of C_{60}/Si (*1*), C_{60}-DT/Si (*2*), C_{60}-Au/Si (*3*) and C_{60}-DT-Au/Si (*4*), λ_{exc} = 488.0 nm, T = 2 K.

known fact that the considerable difference in the reactivity of amines and thiols might influence the cross-linking reaction.

The blueshift has been observed for the PL spectra of both series by lowering the temperature from the room one to 77 K. A further temperature decrease did not induce any distinguishable band shift.

The PL spectra of both series at 2 K demonstrate the clearly defined structure (Figs 7, 8). It should be mentioned the considerable increase of intensity of PL spectra of functionalized and Au-decorated fullerene films in comparison with the intensity of pristine film emission (see Fig. 8). Another peculiarity of the PL spectra of series 2 is the appearance of the band at 1.78 eV. The nature of this band is not quite apparent. Likely, it is caused by some uncontrolled impurities (for example, oxygen).
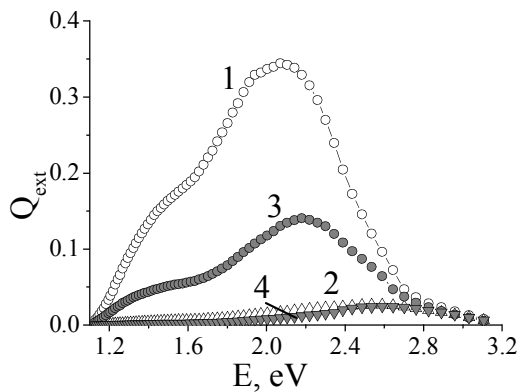
In the low energy range of PL spectra of both series, the band close to 1.52 eV has been carefully observed. The energetic separation with respect to the exciton state at 1.7 eV is about 180 meV. This band can be assigned to the phonon replica involving the high frequency Raman-active mode A_g at 1469 cm^{-1} (182 meV). The Raman spectrum of diamine-

functionalized C_{60} film, obtained earlier [4], showed a decrease of the intensity for the main intramolecular Raman-active modes due to changes in the hybridization state of the diamine-bond carbon atoms in C_{60}.

An example of the spectra of the short-circuit photocurrent, expressed as the external quantum efficiency Q_{ext} (that is, the number of photocurrent carriers generated in metal(Au)/fullerene/Si structure by one photon of the incident light), for the photodiodes including C_{60} layers of the series 1 are shown in Fig. 9. The obtained experimental results can be summarized as follows: (i) the highest photocurrent values were obtained for metal(Au)/C_{60}/Si; (ii) the 1,8-diaminooctane functionalization decreases the photocurrent values by an order of magnitude; (iii) the Ag decoration of fullerene films (especially of pristine C_{60}/Si) also decreases the photocurrent value. To interpret this behavior, the light absorption by the Au and C_{60} layers must be taken into account. The spectra of the internal quantum efficiency Q_{int} (Fig. 10) (that is, the number of current carriers generated by one photon of the light transmitted into Si) were calculated from the experimental Q_{ext} spectra (Fig. 9). Namely, the Q_{ext} values were divided by the corresponding values of light transmitted through metal(Au)/fullerene layers. The photocurrent spectra of the Ag-decorated films are similar in general to ones of the silver-free pristine and diamine-functionalized samples (see curves 1 and 3, 2 and 4 in Fig. 9), but the Q_{int} values for the Ag-decorated samples are considerably lower within the entire spectral range. These calculated Q_{int} spectra take into account the contribution of photocurrent generated in the silicon substrate (including photocurrent, generated outside the diode area). Therefore, the apparent Q_{int} value can be greater than unity. At the same time, the photocurrent generated in the fullerene layer is multiplied by a factor of T_1/T_2 (that is, the ratio of the transmittance T_1 through the Au electrode layer into fullerene to transmittance T_2 through metal(Au)/fullerene layers into Si). Therefore, the contribution of photocurrent generated in the fullerene layer becomes more obvious.

Fig. 7. Photoluminescence spectra of C_{60}/Si (*1*), C_{60}-DA/Si (*2*), C_{60}-Ag/Si (*3*) and C_{60}-DA-Ag/Si (*4*), λ_{exc} = 488.0 nm, T = 2 K.

Fig. 9. Spectra of external quantum efficiency for photodiodes metal(Au)/C_{60}/Si (*1*), metal(Au)/C_{60}-DA/Si (*2*), metal(Au)/C_{60}-Ag/Si (*3*) and metal(Au)/C_{60}-DA-Ag/Si (*4*).
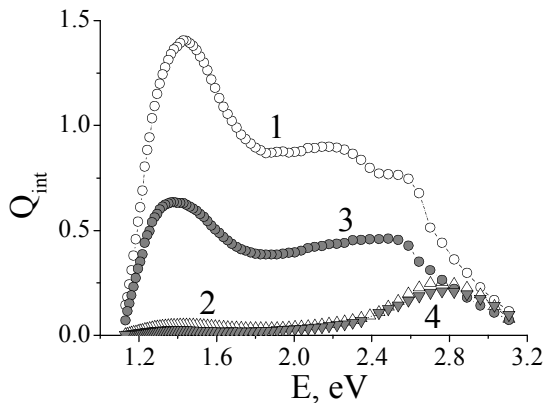
Fig. 10. Spectra of internal quantum efficiency for photodiodes metal(Au)/C_{60}/Si (*1*), metal(Au)/C_{60}-DA/Si (*2*), metal(Au)/C_{60}-Ag/Si (*3*) and metal(Au)/C_{60}-DA-Ag/Si (*4*).

Since the main decrease in Q_{int} for metal(Au)/C_{60}-DA/Si and metal(Au)/C_{60}-DA-Ag/Si is observed within the spectral range of photocurrent generation in the silicon substrate (at energies of < 2.5 eV), this implies a decreased current collection of photocurrent carriers generated in Si. The reasonable causes are the changes in both barrier properties of the fullerene/*n*-Si heterostructure and their recombination characteristics after the 1,8-diaminooctane functionalization. An additional cause of the photocurrent decrease is a certain increase of series resistance of fullerite layer obtained from the analysis of the dark current-voltage characteristics for metal(Au)/C_{60}-DA/Si and metal(Au)/C_{60}-DA-Ag/Si structures as compared to metal(Au)/C_{60}/Si and metal(Au)/C_{60}-Ag/Si, i.e. without diamine treatment. As a whole, the Ag nanoparticle deposition only slightly decreases the light transmittance into the fullerene and Si layers, and has almost no influence on the electrical and photoelectric properties of metal(Au)/fullerene/Si barrier structures. The main influence on the photocurrent is caused by non-radiative recombination in the structure.

4. Conclusions

The method of solvent-free functionalization with 1,8-diaminooctane or octane-1,8-dithiol was employed for the covalent cross-linking of C_{60} thin films capable of binding Ag or Au nanoparticles, respectively. Photoluminescence spectra of the studied nanoparticle hybrid structures have been measured within the wide temperature range (from room temperature down to 2 K). The fine structure of obtained PL spectra is mainly attributed to the recombination of self-trapped polaron excitons and its phonon replicas. The low energy bands are caused by emission from the so-called X traps appearing due to chemical impurities and defects. The changes of recombination properties of fullerene films in consequence of the process of chemical functionalization and decoration with nanoparticles determine the observed changes of PL intensity. The fabricated photodiodes with a semitransparent Au electrode layer onto pristine and functionalized, Ag-decorated and undecorated C_{60} films on n-Si substrate showed a significant decrease of the photocurrent value and some increase of dark resistance for the diamine-functionalized films. These phenomena can be attributed to an insulating effect of 1,8-diaminooctane molecules incorporated between C_{60} cages, which causes a slight change of barrier properties of fullerene/*n*-Si heterostructure and, on the other hand, a considerable increase of the fullerene/*n*-Si interface non-radiative recombination velocity.

References

1. M.S. Dresselhaus, G. Dresselhaus, A.M. Rao, and P.C. Eklund, Optical properties of C_{60} and related materials // *Synth. Metals* **78** (3), p. 313-325 (1996).
2. M.D.R. Taylor, P. Moriarty, B.N. Cotier, M.J. Butcher, P.H. Beton, and V.R. Dhanak, Doping of covalently bound fullerene monolayers: Ag clusters on C_{60}/Si(111) // *Appl. Phys. Lett.* **77**(8), p. 1144-1146 (2000).
3. P.K. Sudeep, D.I. Ipe, K.G. Thomas, M.V. George, S. Barazzouk, S. Hotchandani, and P.V. Kumat, Fullerene-Functionalized Gold Nanoparticles. A self-assembled photoactive antenna-metal nanocore assembly // *Nano Lett.* **2**(1), p. 29-35 (2002).
4. V. Meza-Laguna, E.V. Basiuk (Golovataya-Dzhymbeeva), E. Alvarez-Zauco, D. Acosta-Najarro, and V.A. Basiuk, Cross-linking of C_{60} films with 1,8-diaminooctane and further decoration with silver nanoparticles // *J. Nanosci. Nanotechnol.* **7**(10), p. 3563-3571 (2007).
5. V. Meza-Laguna, E.V. Basiuk (Golovataya-Dzhymbeeva), E. Alvarez-Zauco, T.Yu. Gromovoy, O. Amelines-Sarria, M. Bassiouk, I. Puente-Lee, and V.A. Basiuk, Fullerene C_{60} films cross-linked with octane-1,8-dithiol: preparation, characterization and the use as template for chemical deposition of gold

nanoparticles // *J. Nanosci. Nanotechnol.* **8**(8), p. 3828-3837 (2008).

6. N.L. Dmitruk, O.Yu. Borkovskaya, S.V. Mamykin, D.O. Naumenko, V. Meza-Laguna, E. Alvarez-Zauco, and E.V. Basiuk, Fullerene C60-silver nanoparticles hybrid structures: Optical and photoelectric characterization // *J. Nanosci. Nanotechnol.* **8**(11), p. 5958-5965 (2008).

7. U.D. Venkateswaran, D. Sanzi, A.M. Rao, P.C. Eklund, L. Marques, J.-L. Hodeau, and M. Nuñez-Regueiro, Temperature dependence of the photoluminescence in polymeric solid C_{60} // *Phys. Rev. B* **57**(6), p. R3193-R3196 (1998).

8. Y. Wang, J.M. Holden, A.M. Rao, P.C. Eklund, U.D. Venkateswaran, DeLyle Estwood, R.L. Lidberg, G. Dresselhaus, and M.S. Dresselhaus, Optical absorption and photoluminescence in pristine and photopolymerized C_{60} solid films // *Phys. Rev. B* **51**(7), p. 4547-4556 (1995).

9. N.L. Dmitruk, O.Yu. Borkovskaya, I.B. Mamontova, O.S. Kondratenko, D.O. Naumenko, E.V. Basiuk (Golovataya-Dzhymbeeva), and E. Alvarez-Zauco, Optical and electrical characterization of chemically and photopolymerized C_{60} thin films on silicon substrates // *Thin Solid Films* **515**, p. 7716-7720 (2007).

10. R.W. Lof, M.A. van Veenendaal, B. Koopmans, H.T. Jonkman, and G.A. Sawatzky, Band gap, excitons, and Coulomb interaction in solid C_{60} // *Phys. Rev. Lett.* **68**, p. 3924-3927 (1992).

11. B. Mishori, Y. Shapira, A. Belu-Marian, M. Manciu, and A. Devenyi, Studies of C_{60} thin films using surface photovoltage spectroscopy // *Chem. Phys. Lett.* **264**, p. 163-167 (1997).

12. M. Matus, H. Kuzmany, E. Sohmen, Self-trapped polaron exciton in neutral fullerene C_{60} // *Phys. Rev. Lett.* **68**(18), p. 2822-2825 (1992).

13. W. Guss, J. Feldmann, E.O. Göbel, C. Taliani, H. Mohn, W. Müller, P. Häussler, and H.-U. ter Meer, Fluorescence from X traps in C_{60} single crystals // *Phys. Rev. Lett.* **72**(16), p. 2644-2647 (1994).

14. V.A. Karachevtsev, A.Y. Glamazda, V.A. Pashinskaya, A.V. Peschanskii, A.M. Plokhotnichenko, and V.I. Fomin, Luminescence and Raman scattering of nonpolymerized and photopolymerized fullerene films at 297 and 5 K // *J. Low Temp. Phys.* **33**, p. 704-709 (2007).